Experimental Results on the Design for the APS PID Global Orbit Control System

Jeffrey A. Kirchman and Youngsoo Chung
Argonne National Laboratory
James P. Bobis
Northern Illinois University

Abstract The Advanced Photon Source third generation synchrotron light source needs a stabilized particle beam position to produce high brightness and low emittance radiation. Global orbit correction control is introduced and is utilized to satisfy the demanding needs of the accelerator. This paper presents the experimental results for determining an effective and optimal controller to meet the global orbit correction requirements. These requirements include frequency/time domain demands consisting of vibrational noise attenuation, limiting of controller gains for stability and improving the system time response. Experiments were conducted with a digital signal processor implementing various PID sets to make comparisons between simulations and experiments. Measurements at these PID sets supported the results of software simulation.

I INTRODUCTION

The 7-GeV Advanced Photon Source (APS) at Argonne National Laboratory (ANL) utilizes state of the art technology to produce the brightest beam of high-energy x-rays available for research purposes. The APS storage ring requires stabilization of the particle beam position to achieve the low emittance and high brightness radiation critical to a third generation light source. To achieve this, global and local beam orbit correction feedback is employed [1]. The global feedback control system consists of a PID controller in a digital communication system that collects beam position monitor (BPM) data in digital form, transmits it to a digital signal processor (DSP) and then forwards the resulting power supply correction currents calculated by the DSP to the relevant correctors. This paper presents the experiments that were conducted with a DSP implementing various PID sets to make comparisons between simulations [2] and experiments.

II REQUIREMENTS

The block diagram of the APS closed loop feedback system is shown in Figure 1. The low pass filter (LPF) is designed to provide system stability and to reduce feedback from the noise source. The controller is the PID. The compensation filter (CF) is a derived transfer function that attempts to neutralize the eddy current effects of the magnet and vacuum chamber.
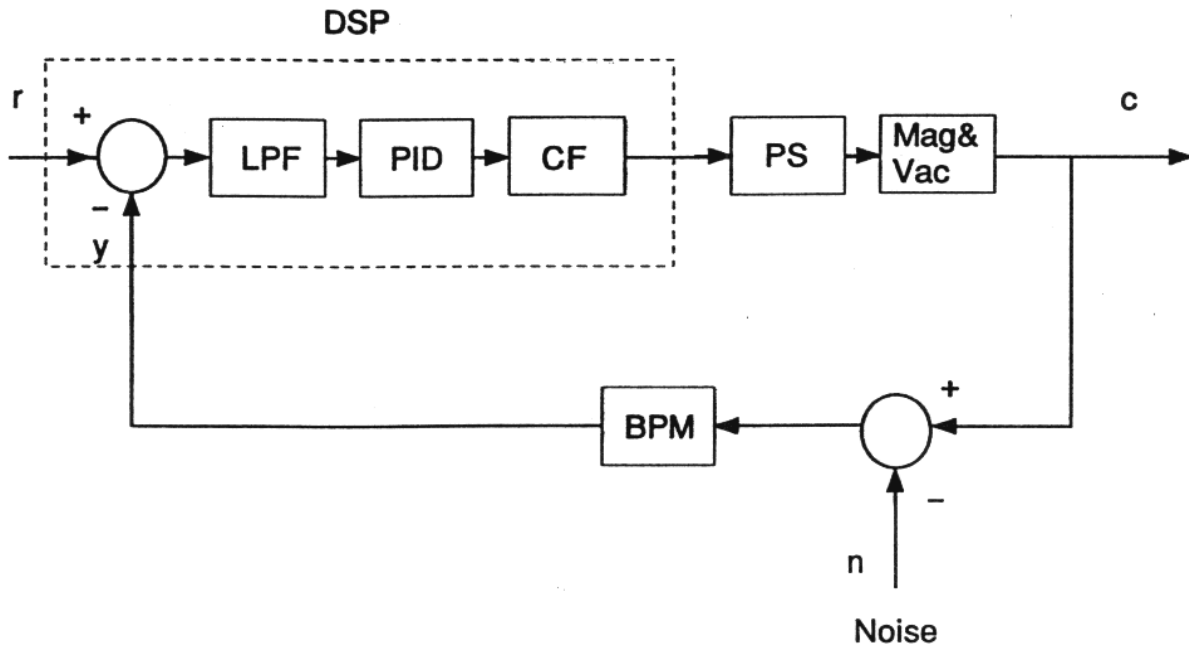

Fig. 1. Simplified block diagram of the APS diagnostic closed loop feedback system

The controller has four main constraints on its design. These are both time-domain and frequency-domain stipulations that should be achieved to allow the closed loop feedback to perform its task. These requirements are:

1. The noise transfer function attenuation should be no less than -12 dB at 20 Hz,
2. The maximum noise transfer function should be less than 2 dB,
3. The system should operate near critical damping to improve time response,
4. The controller gains should be limited to prevent power supply saturation and clipping, which would lead to stability concerns.

The results of the procedure to define a parameter region that satisfies the four main constraints defined by the three gain factors of the PID are shown in Figure 2 [2] where the digital implementation of the PID transfer function is [3]

$$G_c (Z) = K_p + K_i T/Z\text{-}1 + K_d (Z\text{-}1)/TZ$$

and the sampling period is 0.25 ms [2].

The acceptable parameter graph shown in Figure 2 indicates a theoretical practical range of PID parameters to achieve the necessary time and system responses [2]. Various complications can arise in practice that cannot be predicted or compensated. There are numerous areas where these problems can arise; for example the compensation filter designed to cancel the effect of the vacuum chamber, magnet and beam position monitor may perform adequately but not cancel perfectly over the frequency spectrum desired. This in turn would adjust the acceptable ranges of values shown in Figure 2. Other obstacles include temperature, eddy currents, a power supply transfer function that is not truly unity and numerous others which have not been factored into the model. To do so would either be impossible to calculate or would complicate the model to a point of complexity that would make it unusable. Thus simulations may not be entirely accurate, and experiments need to be done to prove the legitimacy of the claims made.
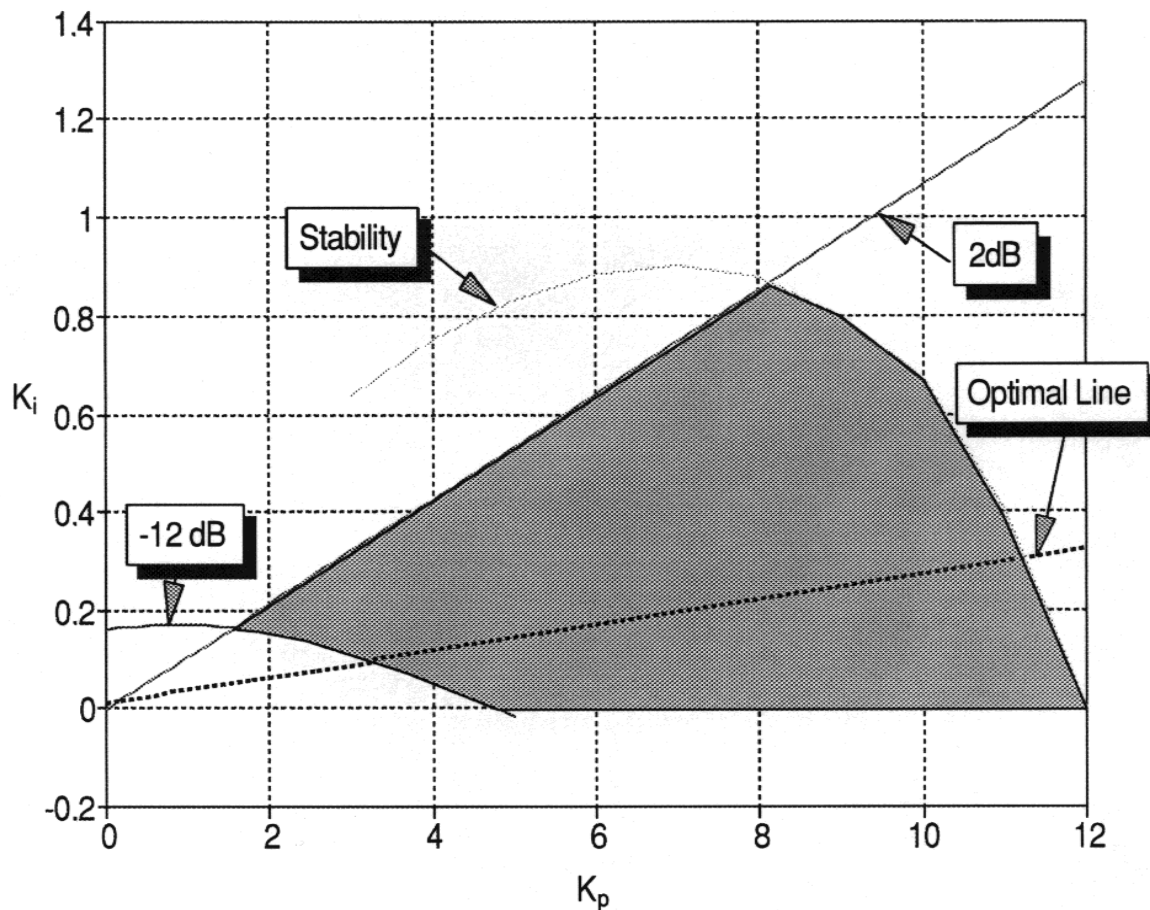
Fig. 2. Acceptable range of parameters for Ki and Kp that satisfy all conditions listed: 20 HZ noise attenuation, maximum noise allowed; system time response and system stability

III EXPERIMENTAL RESULTS

Experiments were conducted using the block diagram shown in Figure 3, the blocks performing the functions of closed loop control. This was implemented using the test setup shown in Figure 4. The DSP completes several tasks in the system. It reduces the bandwidth of the feedback with a low pass filter. This is necessary because the conversion of the analog to digital signals requires the reduced feedback. The low pass filter is anti-aliasing to limit and attenuate the high frequency components. The DSP performs the control portion of the closed loop scheme with a digital PID. It uses the backward rectangular integration digital PID to accomplish this. The final duty of the processor is to compensate for the magnet/vacuum chamber effect in the system.
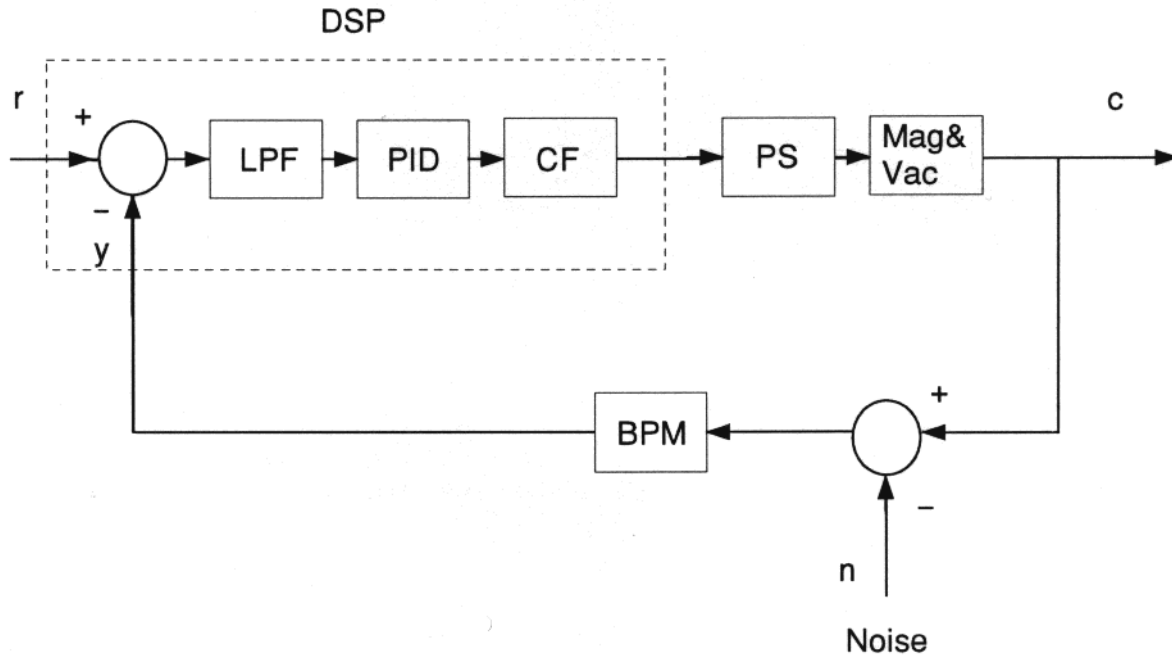

Fig. 3. Block diagram of the actual closed loop system of the global orbit control

Positioned after the DSP is a digital to analog converter on the output. This signal is transmitted to the analog power supply, which for lab experimentation was a Kepco model BOP 20-20M 400 W device. This is a bipolar operational power supply/amplifier capable of being driven by voltage or current and can source or sink 20 A with a voltage capability of 20 V.
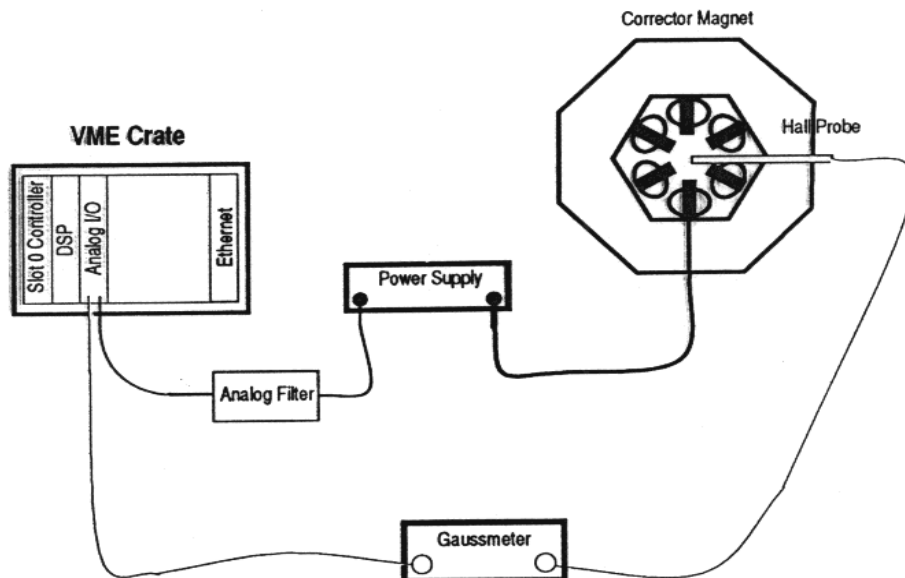

Fig. 4. DSP global orbit feedback test setup

The magnetic field is measured by a Hall effect probe which for purposes of experimentation performs the function of beam position monitor. The beam position is directly affected by the corrected magnet's field, so adequate position simulation is achieved using a probe, together with a gaussmeter, as feedback transducers. This combination measures the magnetic field intensity that reaches the probe through the aluminum alloy vacuum chamber. Eddy currents are formed in this chamber and cause a distortion in the field. This distortion is not static but is dynamically changing, causing difficulty in predicting its transfer function contribution.

The first task performed was the determination of the transfer function for the compensation filter which is in essence the inverse of the magnet/vacuum chamber transfer function. A system analyzer, Hewlett Packard model 3563A, was used to determine this. The analyzer can calculate a digital or analog transfer function for a network by sourcing a test voltage into it and measuring the output. The user may choose the number of poles and zeros in the fit so that a trade-off may be made between fit quality and the complexity and delay required by the filter. The more poles and zeros added the more calculations are needed by the processor, and in general a compromise solution must be accepted.

The first fit contains four poles and three zeros and is depicted in Table 1. The fit is a very good one, and by adding additional poles and/or zeros the response is not significantly improved. The nature of the magnet would lead one to believe that the magnet/vacuum chamber frequency response would have low pass tendencies, and the data and curve fit support this. Since the number of poles is greater than the number of zeros, the net effect is a 20 dB/decade rolloff per unmatched pole for high frequencies.

A different fit contains four poles and two zeros, as is shown in Table 2. This fit does not appear to be so good as the previous one, but the inverted filter does have less gain than in the first case. This is an advantage because the more gain produced by the DSP, the larger the outgoing signal therefore requiring a higher voltage from the power supply, a disadvantage.

The four pole and two zero case becomes a two pole and four zero function when inverted and thus has much gain. Most of this gain appears at high frequencies where there is significant attenuation, but some is placed low enough in the spectrum that it forces the power supply to limit its output. Hence the four pole and three zero curve fit appears to be the better of the two and is the one used for the remainder of this work. Other curve-fit pole/zero combinations were examined, but little was gained by increasing the filter order and much was lost when the order was decreased.

Figure 5 shows the frequency response of both the measured magnet/vacuum chamber and the four pole and two zero digital filter. To cancel the effects of this low pass response of the magnet/vacuum chamber, the digital model filter is inverted to force the product of the two transfer functions toward unity. The ideal case would be unity over the entire frequency spectrum, but since this is extremely difficult frequencies under approximately 1kHz were targeted. That is, more effort went into the design of the compensation filter below 1kHz so that the best compensation would be accomplished in this region. It is for this reason that the number of poles or zeros that are nondominating at high frequency are not critical to the compensation filter design. That design was low order and its performance was adequate with a minimum amount of time delay.
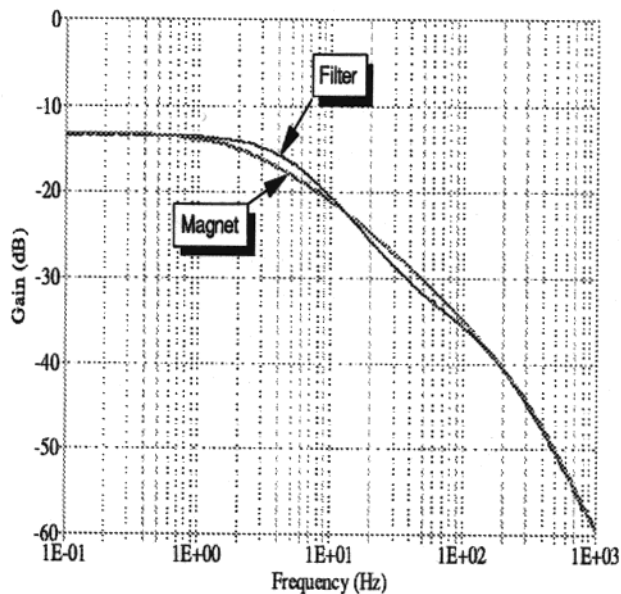
Fig. 5. Frequency response of the digital filter and the actual magent and vacuum chamber

The DSP was programmed with numerous sets of PID values to measure and record the responses. After trying sets of control parameters that ranged from very low to very high gain, it was observed that any set that had

even a modest gain caused the power supply to saturate. One method to alleviate such saturation is the addition of a single pole, low-pass analog filter that helps remove high frequency components which are actually amplified in the controller due to the high-pass compensation filter. For it to truly be a compensation filter, its transfer function had to be the inverse of that for the low pass magnet/vacuum chamber. To cancel the magnet/vacuum chamber transfer function, the compensation filter had then to amplify high frequencies, and approached infinite gain as frequency increased. It could not realistically do this, although it may possess an extremely high amplification in this particular range. This is the justification for the analog reconstruction filter (ARF), which prevents the power supply from limiting due to its inability to switch at that rate.

IV PID INFLUENCE ON ATTENUATION OF NOISE TRANSFER FUNCTION

The first constraint considered is the noise transfer function attenuation, which is a means to measure the ability of the control system to reduce the effects of feedback noise. It is the goal of the control system to have the largest attenuation possible at 20 Hz, below which most vibrational noise is predicted to be present. Figure 6 indicates the PID values used for the experiment.
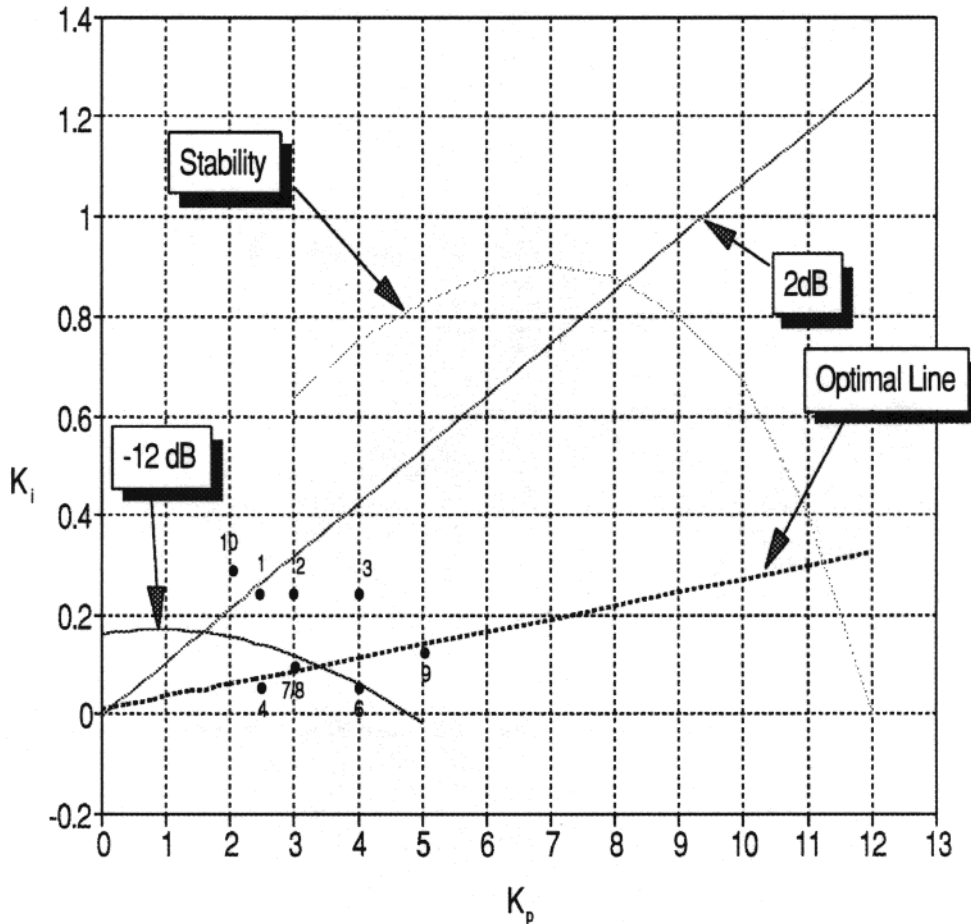

Fig. 6. Points selected to measure system response in the frequency and time domain

The first group of points to be examined are the K_i=0.25 with K_d=0 and K_p ranging from 2.5 to 4.0. This allows analysis of K_p and its impact on noise feedback. Each group of PID sets is subjected to three ARF cutoff frequencies. Figure 7 displays the frequency response of the noise transfer function with K_p=2.5, K_i=0.25, and K_d=0. The three traces shown are taken using this PID with different filter cutoffs. The high frequency noise in the system is readily apparent using a 1000 Hz ARF. The lower frequency range under 1 Hz seems erratic apparently due to the DSP's compensation filter amplifying high frequency noise, and the ARF's cutoff not being low enough to adjust it. The 20 Hz attenuation does not appear to be shaped by the filter. Table 3 shows the frequency results of a series of experiments for ranges of K_p, K_i, and K_d. From this table, all of the first grouping is seen as approximately -18 dB. The second group deviates from a barely unacceptable -11 dB to an adequate -14 dB, depending upon K_p.

(a)   (b)
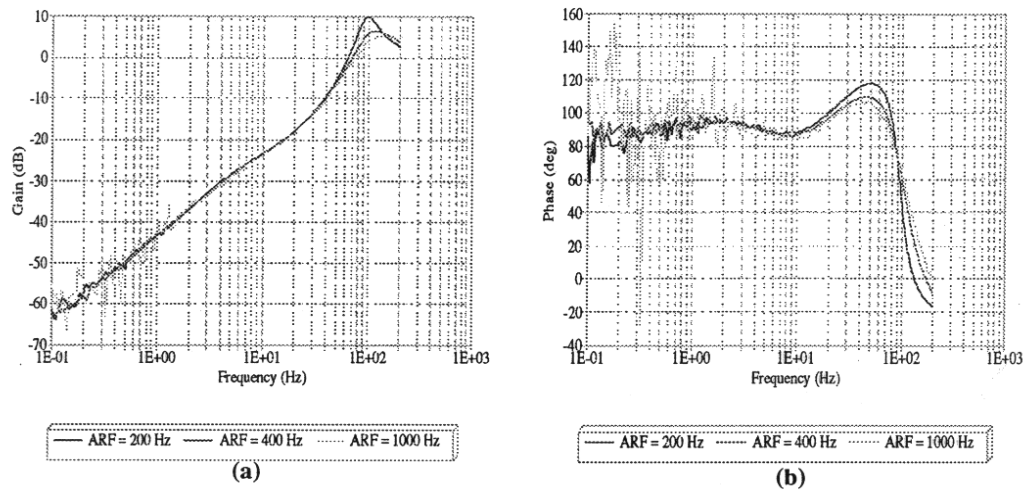
Frequency response of the noise transfer function with $K_p=2.5$, $K_i=0.25$, and $K_d=0$.
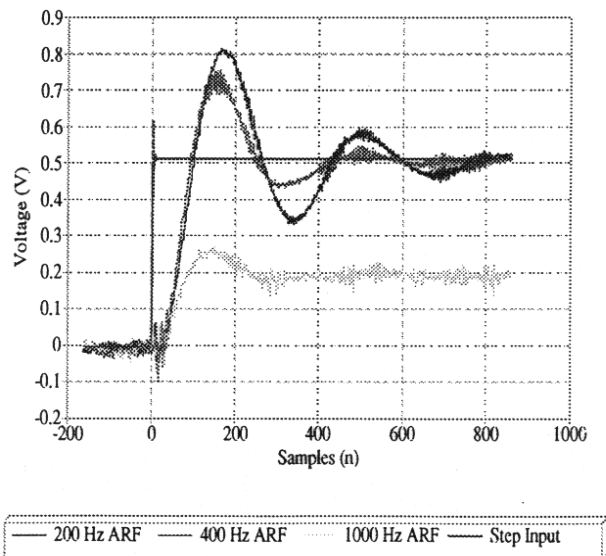
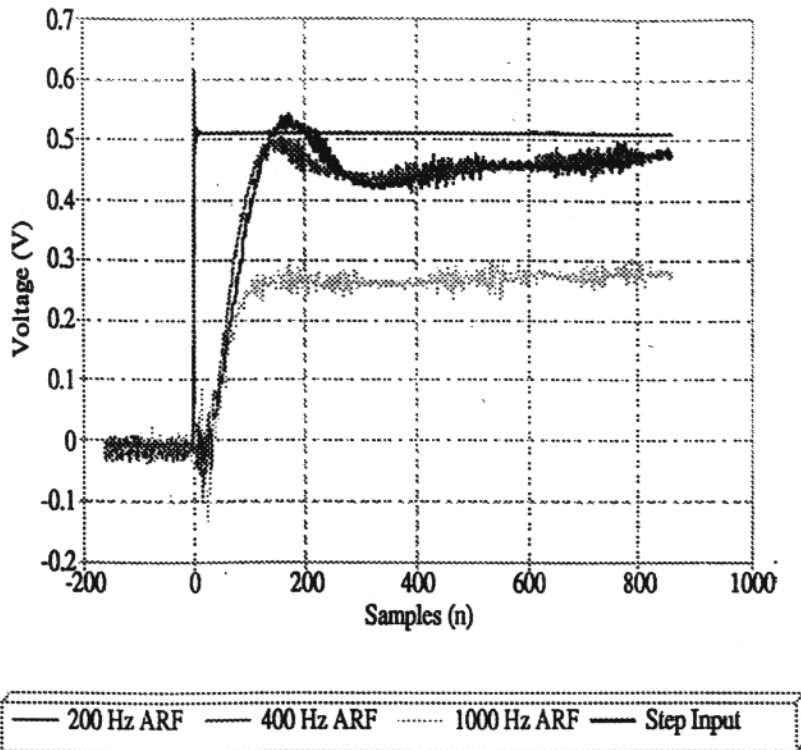**Step response of $K_p = 2.5$, $K_i = 0.25$, and $K_d = 0$.**

Figure 7

Since the proportional and integrative constants are most important, they have received the principal attention. It should be noted that the best attenuation occurred with the last point ($K_p=2$, $K_i=0.3$, $K_d=0$) and the worst with one of the first ($K_p=2.5$, $K_i=0.05$, $K_p=0$). It appears from the table that the integration constant has the

most influence on noise control. It is the integration portion of the PID that gives the closed loop control a pole at DC, so this should be reflected in the value chosen for K_i. It should also be noted that a higher gain assigned to K_p seems to diminish noise. As the gain of G is increased, the effective noise transfer function is decreased. Since the gain of G is directly proportional to the controller proportional constant, any increase in controller gain will reduce noise output.
.

V PID INFLUENCE ON SYSTEM TIME RESPONSE

In a subsequent experiment a step function was applied to the system and by saving the data points stored in the signal analyzer the output response was measured and recorded. The step response was taken using the points of Figure 6 and, as is shown in Figure 7b, the effect of the ARF is apparent. The added pole increases the overshoot and influences the rise time. Because it was necessary to reduce the input signal for the 1000 Hz ARF, it is difficult to compare that case with the other two. It does appear that the 1000 Hz condition has a smaller overshoot than the others, with the 200, 400 and 1000 Hz ARF cases having 60%, 40% and 25% overshoot respectively.

Examination of Figures 8 and 9 reveals more about the system time response. The value of K_i has been reduced from 0.25 to 0.05 and this has changed the step response significantly. When the proportional constant K_p is 2.5 the system response is slightly underdamped with minimal overshoot. However as K_p is increased the overshoot and settling time escalate. This indicates that decreasing the integrator gain K_i while increasing the proportional gain does not diminish the overshoot.

Figure 8 Step response of $K_p = 2.5$, $K_i = 0.05$, and $K_d = 0$.
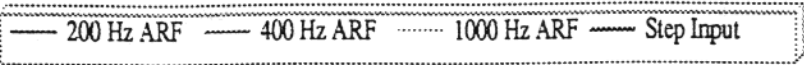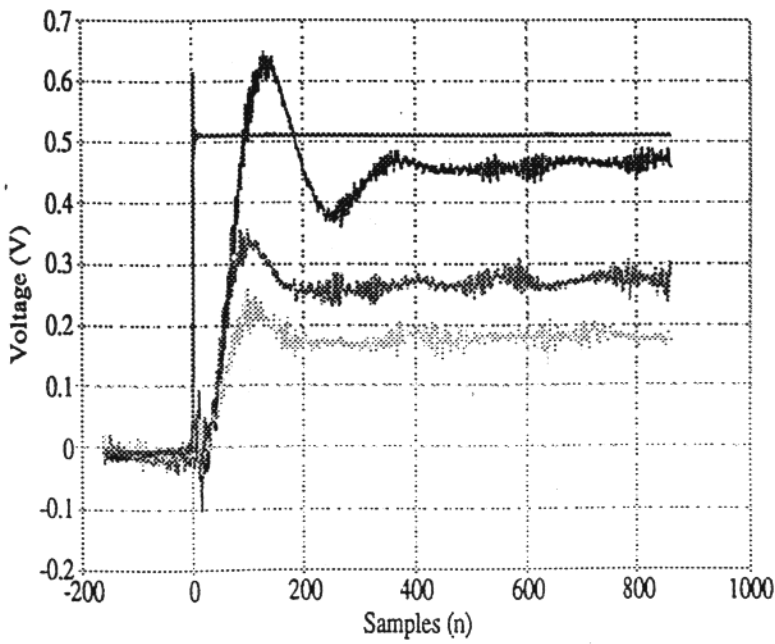
Figure 9   Step response of $K_p = 4$, $K_i = 0.05$, and $K_d = 0$.
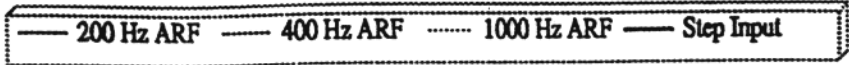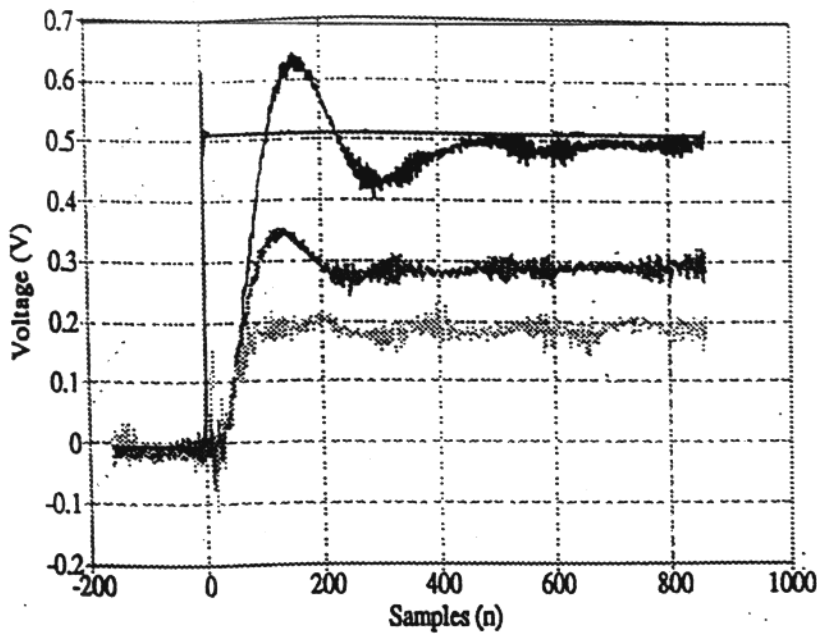
Figure 10   Step response of $K_p = 3$, $K_i = 0.1$, and $K_d = 0$.

What happens if derivative control is utilized to help offset integration control is indicated in Figures 10 and 11. Using values of $K_p =3$, $K_i =0.1$ and K_d either 0, no control, or 1, one can see that without derivative control the 200 Hz ARF overshoot is approximately 25%, but with it the overshoot decreases to 20%, not a huge benefit but an

advance nonetheless. With the 400 Hz ARF a more pronounced change in that response appears, being converted from underdamped to critically damped.
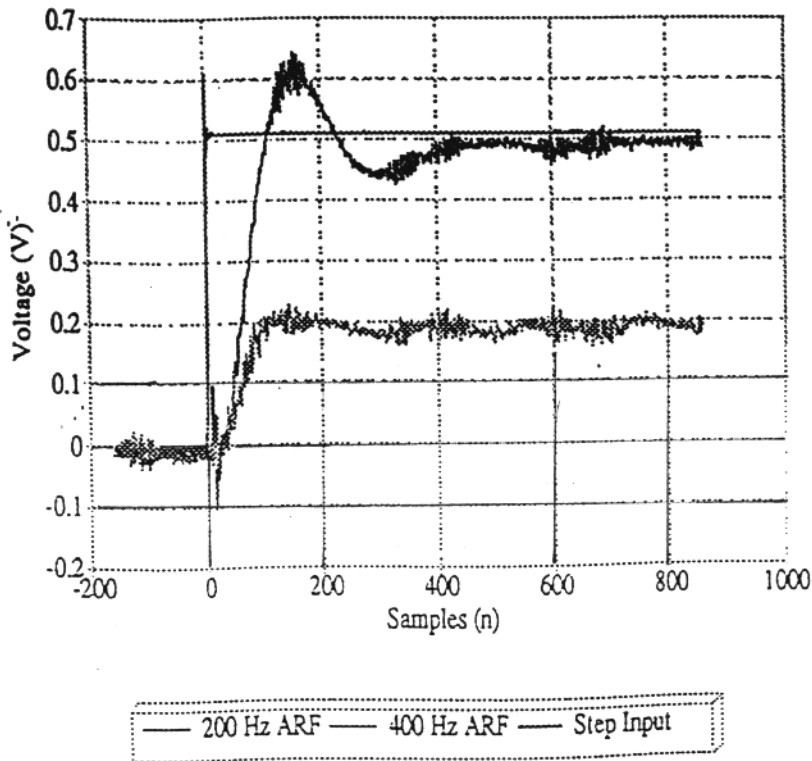
Figure 11   Step response of $K_p = 3$, $K_i = 0.1$, and $K_d = 1$.

Table 1 Filter coefficients of the first compensation filter design.

$a_0 = 9.41294 \times 10^{-4}$ $b_1 = -1.87602$
$a_1 = 1.30784 \times 10^{-2}$ $b_2 = 7.05058 \times 10^{-1}$
$a_2 = -8.52438 \times 10^{-4}$ $b_3 = 3.46876 \times 10^{-1}$
$a_3 = -1.11792 \times 10^{-2}$ $b_4 = -1.74941 \times 10^{-1}$

$$H(z) = \frac{\Sigma a_k z^{-k}}{1 + \Sigma b_k z^{-k}}$$

Table 2 Filter coefficients of the second compensation filter design.

$a_0 = 1.36339 \times 10^{-2}$ $b_1 = -2.87463$
$a_1 = -7.6617 \times 10^{-4}$ $b_2 = 7.16485 \times 10^{-1}$
$a_2 = -1.091 \times 10^{-2}$ $b_3 = 3.25489 \times 10^{-1}$
                                        $b_4 = -1.66391 \times 10^{-1}$

$$H(z) = \frac{\Sigma a_k z^{-k}}{1 + \Sigma b_k z^{-k}}$$

Table 3 Noise transfer function measurements including maximum gain, frequency of maximum gain, 20 Hz attenuation, and phase margin.

K_p	K_i	K_d	ARF	sweep	G_{pk}	f_{pk}	G@20Hz	P.M.
1	0.25	0	200	200	10	98	-18	114
			400	200	6	119	-18	99
			1000	200	5	119	-19	89
3	0.25	0	200	200	9	108	-18	109
			400	200	6	130	-18	93
			1000	200				
4	0.25	0	200	200	9	143	-19	104
			400	200				
			1000	200				
1	0.05	0	200	500	4	125	-11	60
			400	500	4	172	-11	51
			1000	500	3	202	-11	45
3	0.05	0	200	500				
			400	500				
			1 000	500				
4	0.05	0	200	500	7	147	-14	75
			400	500	6	202	-14	64
			1000	500	6	202	-14	59
3	0.1	0	200	200	6	124	-13	75
			400	200	6	124	-13	63
			1000	200	7	113	-14	61
3	0.1	1	200	200	6	124	-13	70
			400	200	6	124	-14	59
			1000	200	6	119	-13	64
5	0.125	0	200	200	7	173	-16	88
		0	200	200	7	173	-16	87
		1	200	200	7	165	-16	88
2	0.4	0	200	200	8	81	-22	152
		0	200	200	8	81	-22	149
		1	200	200	8	81	-22	148

The most important questions are: Did the simulation tests support the data taken for the actual time responses? Does the optimal line live up to its name? If the 1 kHz ARF cases are examined and compared the optimal line seems to hold true. However it is important to realize that the 1 kHz ARF case is closest to simulation conditions where there actually was no analog reconstruction filter. The 1 kHz cutoff puts the pole far enough away from the rest of the response that its influence is not great.

The points 4, 7,8 and 9 of Figure 6, nearest the optimal line, display little or no overshoot with the exception of point 9. This point uses a 200 Hz ARF, which has adversely influenced the response to reflect the added pole. Since the other two points on this line approach critical damping, there is no other reason for point 9 to do so. These other points also have excellent rise times and settling times, while if one deviates from this optimal line the effects can be readily seen.

VI CONCLUSION

The APS third generation synchrotron light source requires a global orbit control system that reduces noise effects and stabilizes the beam. This was accomplished through a high speed feedback loop established completely around the accelerator ring. This encompassing control system requires a specific kind of control that balances its needs without compromising any of these demands too heavily.

The need exists for a controller to achieve noise reduction, but other consequences must be considered as well. Such notable system attributes as time response, stability, power supply bandwidth and cost are all concerns of closed loop control and it was necessary to find a control algorithm that met or exceeded the design criteria. The PID controller proved to be the best in this situation, and design centered on the choice of proportional, derivative and integral gains and sampling time

Experimentation has justified the type of controller design, where optimal control was achieved using three-dimensional plots of the performance in question. These plots were constructed with two of the design parameters as variables; they can also be organized into tabular format to facilitate comparison viewing. The performance measures were rated in terms of noise filtering ability, system response time or system stability. This paper has described methods to assess system performance of both time and frequency domain functions.

Performance of noise rejection was measured by plotting the noise transfer function value at a critical frequency for different values of K_p, K_i, and K_d where the values that met or exceeded the criterion for handling injected noise were plotted. The same procedure holds true for determination of maximum gain of the noise transfer function.

The work performed in this paper examined the controller's design effects on the performance of the system with one "BPM" and one corrector. A better experiment could be performed using all 40 of the BPMs and correctors. This would be the final proof of the efficiency and capability of the controller design. This experiment would need to be performed on an existing accelerator where a PID loop could be programmed into a global orbit feedback system.

REFERENCES

1. D.Bulfone et al., "Design Considerations for the ELETTRA Beam Position Feedback Systems," European Particle Accelerator Conference, 1990, PP 895-897.

2. J. A. Kirchman and J.P. Bobis, "Preliminary Design of the APS PID Global Orbit Control System," IEEE International Conference on Industrial Electronics, Control and Instrumentation, Maui, Hawaii, Nov. 1993.

3. Benjamin C. Kuo, Automatic Control Systems, Prentice-Hall, Englewood Cliffs, NJ 1991.